

Assessment of the Planar Low Power Discrete *nnpn* Structure Radiation Hardness Under γ -irradiation Taking into Consideration Non-linear Change of the Holding Current Probability

Sergey BYTKIN

Department of Electronics, Information Systems and Software Development of Engineering
Educational and Scientific Institute named after U. M. Potebnja of Zaporizhzhya
National University, Zaporizhzhya, pr. Sobornyj, 226, Ukraine
Tel.: +38 (096)7128400
E-mail: sergey.bytkin@gmail.com

*Received: 13 March 2024 / Revised: 10 November 2024 / Accepted: 11 December 2024
Published: 30 December 2024*

Abstract: The radiation degradation of the *nnpn* thyristor radiation-sensitive characteristic, holding current, I_{holding} , considered. As the dose of γ -irradiation (Φ_γ) increased, the distribution of the I_{holding} shows pulsating change (quasi-periodicity) in quantity and amplitude of peaks (extremes) of I_{holding} in a wide range of Φ_γ . The investigated thyristors samples show real radiation hardness only up to 200 mSv. At $200 \leq \Phi_\gamma \leq 1000$ mSv I_{holding} S-shape degradation was observed. From a practical point of view, using such a low-power discrete planar *nnpn* thyristor in the range of $1000 \leq \Phi_\gamma \leq 7 \cdot 10^3$ mSv is advisable. For the range of approximately $6 \cdot 10^3 \leq \Phi_\gamma \leq 1 \cdot 10^5$ mSv it's difficult to forecast the value of the I_{holding} (heavy risk zone). $\Phi_\gamma \geq 1 \cdot 10^5$ mSv may be considered a failure zone of the devices. The evaluation method was proposed for a realistic assessment of the radiation resistance of discrete devices. It includes the construction of approximating I_{holding} dose dependence using results of experimental measurements and calculations to find laminar (smooth) and chaotic (jagged) phases of degradation. The laminar phase will show the ranges of real radiation hardness (no changes of the holding current) and predictable changes of device parameters under irradiation. The beginning of the chaotic phase indicates the end of the reliable *nnpn* structure operation and the possibility of soon device failure. Obtained experimental results agree with previously received theoretical approaches of other authors.

Keywords: Low power *nnpn* structure, γ -irradiation, Bimodal distribution, Probability, Radiation hardness, Heavy risk zone, Failure, Phases of the holding current degradation, Realistic assessment of the radiation resistance of discrete devices.

1. Introduction

A severe nuclear power plant (NPP) accident can release significant radiation from the reactor core [1]. For example, the Chernobyl disaster exposed a substantial fraction of core material to the environment. The exposed reactor created γ -radiation; the highest dose was about 300 Sv/h. Similarly, the Fukushima disaster also released many radioactive substances into the environment due to hydrogen explosions and fire damage to the containment structures. In Feb. 2017 the level of radiation was estimated to be up to 530 Sv/h. So, the design of radiation-hardening methodologies, as well as rad-

hardened analysis techniques are not a luxury, but necessary, to ensure the reliable operation of the special equipment (post-accident monitoring systems (PAMs), mobile military robots) to work in harsh environmental conditions during decommissioning processes in the event of an accident. Approach, based on the rad-hardened components employed for special-purpose equipment manufacturing can be excessively expensive due to special semiconductor materials used, technology complexity in the production processes, and most of all, the small size of the market supporting such devices. Another approach is to rely on regular commercial off-the-shelf (COTS) devices with high vulnerability to radiation.

Experience in the use of "extreme robotics" in the external conditions of a radiation accident, for example, during cleaning of the destroyed reactor from highly radioactive elements, debris of the structure, fuel residues etc. (γ -background level up to ≈ 3000 Roentgen per hour (R/hour), in some places, radiation levels up to $\approx 10^4$ R/hour), showed the possibility of decontamination using a mobile robot, on which all drives were made electromechanical [2]. Control systems were made on very humble relay elements. It is not possible for complicated intelligent robotic systems [3, 4]. Therefore, the radioactive shielding protection of the radiation-sensitive robot components is now considered the key technology of robot efficiency in severe radiation ambiance. Still, protecting the mobile platform and manipulator sufficiently increases the robot's weight, thus affecting its motion flexibility [5] near the destroyed reactor, creating the risk of lodging. Reducing the thickness of protection enhances robot survivability in hazardous radiation environments. For highly complex work, it is necessary to use solid-state relays (SSRs), because of various features that mechanical relays do not incorporate [6]. SSRs are immune to the shock and vibrations at levels, normally encountered [7]. This facility employs semiconductor switching elements, transferring the signals at high frequency. Most DC solid-state switching devices commonly use power transistors, whereas, for an AC SSR, the switching device is either a triac or back-to-back thyristors instead of the usual mechanical normally open contact relays [8]. Thyristors are preferred due to their high voltage and current capabilities. Theoretically, it is necessary to increase the radiation hardness of electronic components to complete the equipment to eliminate accidents at nuclear power stations with an element component base operating at γ -irradiation with an intensity of up to 10 R/s and an integral dose of up to 10^6 R [9]. This is a technologically complex task [10]. The radiation-hardening methodology, Rad-Hard-By-Process (RHBP), employs modified manufacturing processes to improve their ability to withstand radiation. The cost of developing new RHBP became prohibitively expensive; as a result, there are no widely used industrial technologies [11]. That's why creating new approaches to radiation hardness improvement is stably relevant.

2. The Purpose of the Work

The evolution of the structure of radiation damage of the irradiated objects (and semiconductor devices, of course) is also accomplished, under certain stationary irradiation conditions radiation defects density self-organizing [12]. Many experimentally observed phenomena that correspond to self-organization, such as self-oscillations of conductivity, non-monotonous dose dependence of microhardness, non-monotonous dose dependence of creep, oscillations of the size of vacancy voids, etc.

due to the probability of their sensitive characteristics changing to much higher or lower values than expected before irradiation.

Therefore, it is necessary to consider the possibility of self-oscillation, for example, of the thyristor characteristics for the secure operation of nuclear facilities. For the confident operation of discrete devices in a hazardous radiation environment, it is necessary to consider the possibility of the most thyristor radiation-sensitive characteristic – holding current (I_{holding}) – self-oscillation.

The possibility of applying theoretical concepts of self-organization in the analysis of experimental data obtained by irradiation of low-power npnp thyristors was proposed in [13]. Shown, that as the dose of γ -irradiation (Φ_γ) increased, the distribution of the I_{holding} shows pulsating change (quasi-periodicity) in quantity and amplitude of peaks (extremes) of I_{holding} in a wide range of Φ_γ . At the same time, this work did not investigate the dependence of the reproducibility of experimental results on the radiation dose, i.e. dispersion of I_{holding} . It is also necessary to describe the calculation methods that allow reflection the specific features of the thyristor degradation (laminar (smooth) and chaotic (jagged) phases).

Thus, the purpose of the present work was to receive details of the npnp structure I_{holding} radiation degradation to find possible ties with radiation-induced self - organization processes.

3. Devices (npnp Structures), Method of Measurement

The description (vertical structure, package, geometric dimensions) of the used experimental low-power thyristors is given in [14].

Measurements were carried out by [15]. The isotope Americium-241 (the half-life 432.6 years) with the following main parameters: energy of γ -quanta $E = 59.5$ keV; photon flux density at a distance of 1 m from the center of the working surface $(7.0 \pm 2.1) \cdot 10^4 \text{ s}^{-1} \text{ cm}^{-2}$; maximum activity of the source 2.24 Ku used as a source of γ -radiation [16].

4. Results of Experiment

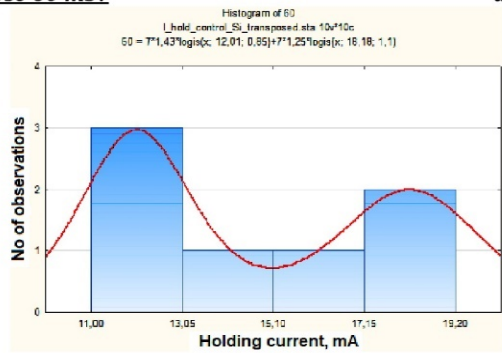
4.1. Quasi-periodic Change in the Numerical Value of the Holding Current Probability of a Low-power npnp Thyristor under γ -Irradiation

The results of the holding current measurements were analyzed using Statistica 10 [17]. The nonlinear relationship between Φ_γ and the number of peaks with different forms and amplitude was experimentally observed (Fig. 1). Formulas of used distribution density functions (e is the base of the natural logarithm (2.71), π is the constant Pi (3.14) are in the cells with

histograms in Fig. 1. It was discovered that as the dose of γ -irradiation increased, the distribution of the thyristor sample selection distribution modes, and the

amplitude of the peaks of I_{holding} , did not change monotonically.

Dose 60 mSv

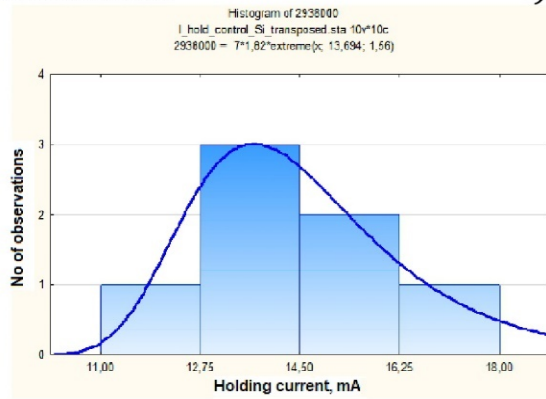


logis (x, a, b) the logistic distribution:

$$f(x) = \frac{1}{b} \cdot \exp\left(-\frac{(x-a)}{b}\right) \cdot \left[1 + \exp\left(-\frac{(x-a)}{b}\right)\right]^{-2}$$

where a is the mean of the distribution,
 b is the scale parameter

Dose 293800 mSv



extreme (x, a, b) – the extreme value distribution:

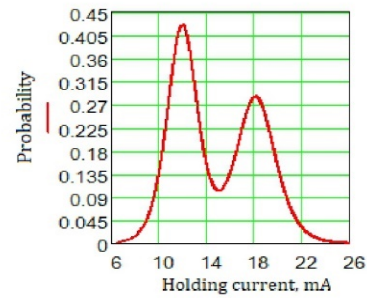
$$f(x) = \frac{1}{b} \cdot \exp\left(-\frac{(x-a)}{b}\right) \cdot e^{-e^{-\frac{(x-a)}{b}}}, \text{ where}$$

a is the location parameter, b is the scale parameter
of the distribution; $b > 0$ e)

b)

The Probability of the Holding Current at the dose of 60 mSv

$$\begin{aligned} \text{Probability}_{I_{\text{hold_Si}}60}(I_{\text{hold_Si}}) &= \\ &= 1.43 \cdot \text{dlogis}(I_{\text{hold_Si}}, 12.01, 0.85) + \\ &+ 1.25 \cdot \text{dlogis}(I_{\text{hold_Si}}, 16.18, 1.1) \end{aligned}$$



d)

The Probability of the Holding Current at the dose of 293800 mSv:

$$a_{I_{\text{hold_Si}}293800} = 13.694, b_{I_{\text{hold_Si}}293800} = 1.56,$$

$$\text{Probability}_{I_{\text{hold_Si}}293800}(I_{\text{hold_Si}}) =$$

$$\begin{aligned} &= 1.82 \cdot \frac{1}{b_{I_{\text{hold_Si}}293800}} \cdot \\ &\cdot e^{-\frac{I_{\text{hold_Si}} - a_{I_{\text{hold_Si}}293800}}{b_{I_{\text{hold_Si}}293800}}} \cdot \\ &\cdot e^{-e^{-\frac{I_{\text{hold_Si}} - a_{I_{\text{hold_Si}}293800}}{b_{I_{\text{hold_Si}}293800}}}} \end{aligned}$$

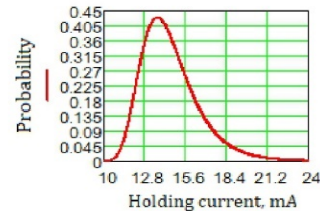


Fig. 1. Examples of the Distributions of Numerical Values of the Holding Current at Different γ -irradiation Doses.

With an increase in the radiation dose, there is a periodic increase/decrease in the probability of I_{holding} in a wide range of numerical values, Fig. 2.

This phenomenon is characteristic of irradiation of solids [18] (including, in our opinion, npnp crystal structures of silicon discrete low-power thyristors), which in this case are the so-called open flow-type system. The energy flux of γ -irradiation, which does not dampen in a certain interval, maintains conditions in the irradiated sample far from thermal equilibrium. As a result of radiation exposure, the structure of the semiconductor material of the irradiated thyristor is disrupted due to the formation of radiation defects. As the radiation dose accumulates, the structure of radiation damage in Si becomes more complex. The phenomena occur due to various interrelated

processes, among which it is often impossible to single out several dominant ones (the phenomenon of synergy). Mobile defects (vacancies, first of all) can form clusters (in particular, clusters of divacancies) and bind into electrically active complexes (A-, E-, K-centers) with impurity atoms. As a result, their spatially ordered concentration distribution (stratification) is formed, which depends on the radiation dose (which, in turn, depends on the exposure time).

Each accumulated radiation dose probably corresponds (to some extent) to an *individual* [14] distribution of impurity-defective complexes. At the same time, it is logical to assume that there is a quasi-periodic reproduction of the structure of the recombination regions of the npnp structure created by

radiation exposure. This partly causes a "pulsating" change in the probability of the numerical value of the thyristor holding current during irradiation.

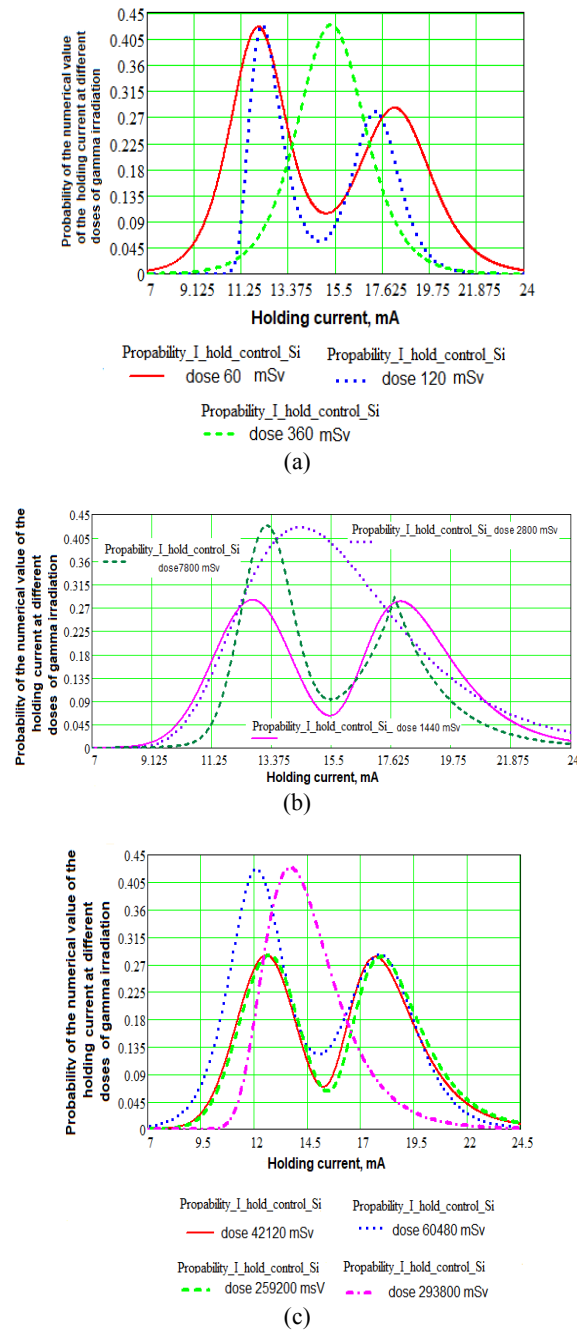


Fig. 2. Quasi-periodic change in the probability of the numerical value of the I_{holding} under γ -irradiation.

So, the evolution (change) of the dependence of probability fluctuations of the I_{holding} in a wide range of radiation doses can be considered a reflection of the self-organization of complexes of radiation defects.

In other words, at certain doses of γ -irradiation, the distribution of the I_{holding} becomes more *homogeneous* (Fig. 2(a)) $\Phi_\gamma = 360$ mSv; b) 2800 mSv; c) 293800 mSv); it may reflect the similar distribution of impurity-defective complexes in the irradiated Si single crystal on which the npn structure is formed.

From a practical point of view, the shape of the resulting oscillations of the I_{holding} is consistently reproducible, albeit at different Φ_γ values (Fig. 3).

For certain doses, *modes*, most likely values of peaks of Holding Currents *probabilities*, are in relatively narrow intervals of the numerical values of the I_{holding} .

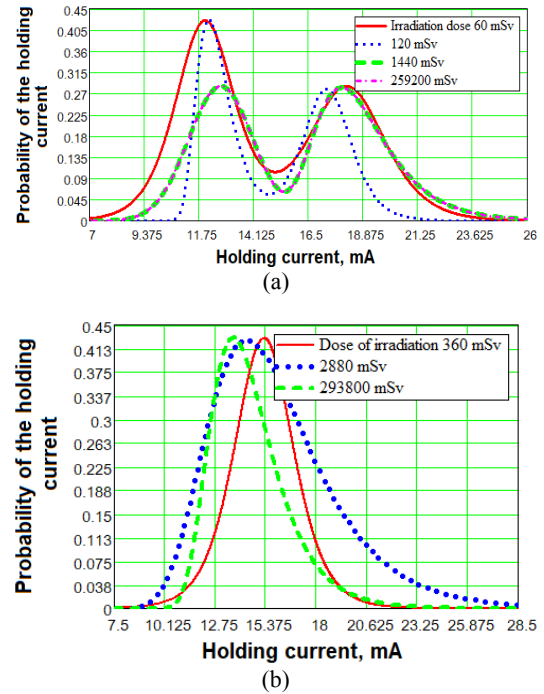


Fig. 3. The probabilities of different numerical values of I_{holding} , grouped by the shape of their probability distributions; a) –bimodal; b) –unimodal distributions.

Self-organization can also be understood as periodic (similar to pulsating) associated with an increase in Φ_γ , a change in the number and amplitude of peaks of the I_{holding} , observed at different doses of radiation (Fig. 4, Left axis). In addition, there is a periodic change in the difference (Δ) (Fig. 4, Right axis) numerical values of peak amplitudes, including $\Delta = 0$ observed for the same defined values Φ_γ , in which the distribution of the I_{holding} is unimodal.

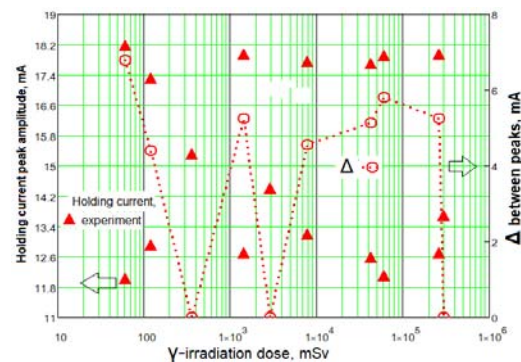


Fig. 4. Pulsating change in the amplitude of peaks (extremes) of I_{holding} in a wide range of Φ_γ .

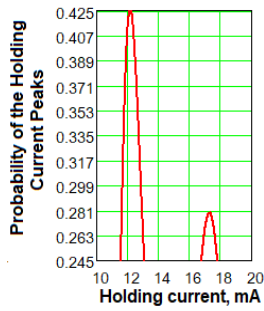


Fig. 5. A pronounced difference in the amplitudes of the left (extreme distribution) and right (logistic) extremes (peaks) of the Holding Current at $\Phi_\gamma = 120$ mSv.

The same calculations were made for every value of the *probability of I_{holding} peak* at different Φ_γ , Fig. 6.

60	12.01	0.4206
60	18.18	0.2842
120	12.9	0.425
120	17.3	0.281
360	15.3	0.429
1440	12.7	0.285
1440	17.95	0.283
2880	14.4	0.425
7800	13.185	0.428
7800	17.75	0.292
42120	12.57	0.2855
42120	17.7	0.2824
60480	12.1	0.419
60480	17.9	0.286
259200	12.7	0.285
259200	17.95	0.282
293800	13.694	0.43

$I_{\text{hold_peaks_control_Si}} :=$
 $\Phi_\gamma := I_{\text{hold_peaks_control_Si}}^{(0)}$ [mSv]
 $I_{\text{hold_peaks_Si}} := I_{\text{hold_peaks_control_Si}}^{(1)}$ [mA]
 Prob I hold peaks Si := I hold peaks control Si⁽²⁾

Fig. 6. Experimental results for visualization of the value of the probability of I_{holding} peaks at different Φ_γ

Increasing the radiation dose Φ_γ in the studied range leads to a decrease in the likelihood of I_{holding} peaks with a high amplitude, and, accordingly, an increase in the possibility of peaks with a lower amplitude of I_{holding} when enlarged Φ_γ . For certain ranges of Φ_γ , the effect of the maximum of I_{holding} peaks probabilities exists, Fig. 7.

Using MathCAD shows *two* numerical values of Φ_γ , in which the so-called "effect of small doses" [19] is observed, Fig. 8.

Reduced probability of high-amplitude currents means longer (increased) lifetimes of minority charge carriers τ_p in the wide thyristor n-base after irradiation by $\Phi_\gamma \approx 4.2 \cdot 10^4$ mSv. Data in [20, p. 55] confirms that the relatively low *increase* in τ_p leads to a significant *decrease* in I_{holding} . The physical cause of the increase in τ_p is the transition of the crystal to an equilibrium state, which is considered to be when irradiated with small doses of γ -quanta. This is accompanied by a significant change in their electrophysical properties: an increase in the lifetime and mobility of charge

carriers. Observed in a certain range of ionizing radiation doses, τ_p increases significantly due to the ordering of the structure of the crystal lattice of silicon. This is possible only by releasing the energy stored in the crystal [21].

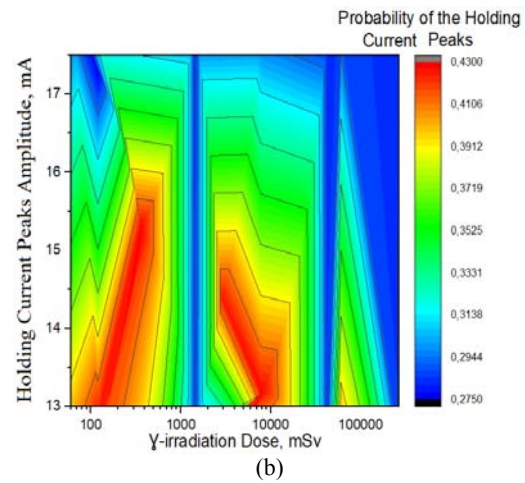
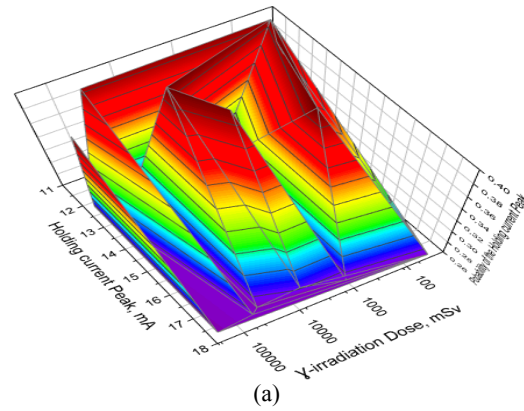


Fig. 7. The probabilities of different ranges of numerical values of I_{holding} peaks, grouped by γ -irradiation doses (Origin PRO); a) 3d visualization, b) contour plot.

The process of energy storage is simplistically considered as the process of increasing the internal energy of a physical system (e.g., npnp structure), regardless of how this energy was increased (added), including, obviously, as a result of the diffusion technology of the thyristor.

According to the authors of the cited works, the effect's physical essence lies in the relaxation of energy stored in the form of defects in the crystal. Heat is released due to the annihilation of defects in the crystal lattice of a solid body during its transition to an equilibrium state in the irradiation process.

At $\Phi_\gamma \approx 4.2 \cdot 10^4$ mSv ("small dose") there is a decrease in the probability of observing amplitude hold-current peaks range 13.6...18 mA ("high currents") from 0.411 to 0.304 or by ≈ 25.8 % (better seen in Fig. 9).

For the peaks of I_{holding} with the amplitudes 12...13.5 mA ("low currents") the reduction in their probability at this radiation "small dose" is about

2.14 % (from probability ≈ 0.42 to 0.411) or almost an order of magnitude less than for the "high currents". Range $\approx 6 \cdot 10^4 \leq \Phi_\gamma \leq 1.8 \cdot 10^5$ mSv is relatively homogeneous in terms of a smooth change (decrease) in the probability of I_{holding} in the range 12...18 mA. The most probable value of holding current in the range $10 \dots 2.5 \cdot 10^5$ mSv is $I_{\text{holding}} = 13.5$ mA (probability of this holding current $\approx 0.42 \dots 0.304$ changes in a wide range, but the line $I_{\text{holding}} \approx \text{const} \approx 13.5$ mA practically connects the mountaintops of the "canyon" regions, i.e. the regions of holding current, in which a pronounced instability of the probabilities of the I_{holding} peaks is observed. It may be considered, in this case, as the border between "high" and "low" amplitude values of the holding current.

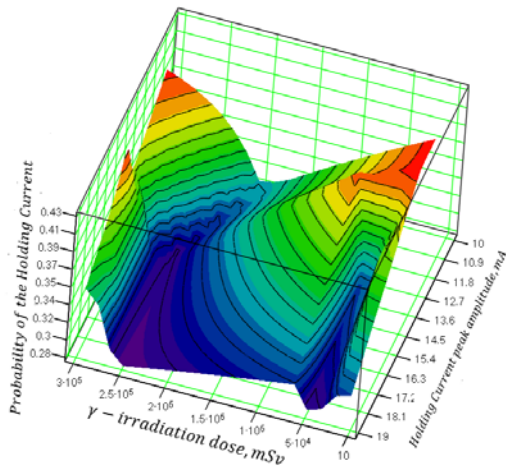


Fig. 8. Probabilities of Different Numerical Values of the Holding Current Peaks at Different γ -irradiation Doses; 3d visualization.

For $I_{\text{holding}} \geq 13.5$ mA, i.e., in the region with a less ordered structure, a **decrease in the probability of the amplitude of hold-current peaks is observed once more** at $\Phi_\gamma \approx 2.47 \cdot 10^5$ mSv, Fig. 9. This dose is

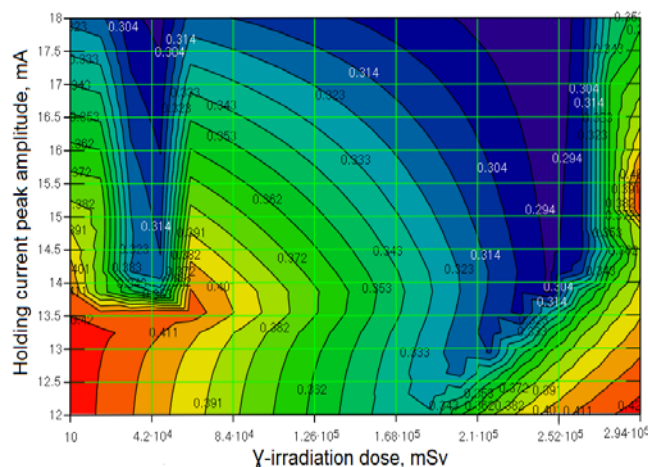


Fig. 9. Probabilities of Different Numerical Values of the Holding Current Peaks at Different γ -irradiation Doses; contour plot.

in the usually considered range of "low doses" of irradiation, ($10^4 \dots 10^5$ R $\approx 100 \dots 1000$ Sv = $1 \cdot 10^5 \dots 1 \cdot 10^6$ mSv).

So, the dose $\Phi_\gamma \approx 4.2 \cdot 10^4$ mSv may be considered "ultra-low". This effect for the thyristor sample under consideration is manifested in the range of amplitudes of the holding current peaks $13.5 \leq I_{\text{holding}} \leq 18$ [mA]. Observation of the "low-dose effects" concerning peak amplitudes of I_{holding} allows reasonable selection of the criterion for rejection of npnp structures for sampling before radiation resistance tests. There is no point in testing knowingly unstable devices [22] with $I_{\text{holding}} > 13.5$ mA under the influence of γ -radiation.

4.2.2. Effect of γ -irradiation Dose on all Current Values of I_{holding}

There is an alternation of extremes (zones of max and min values of I_{holding}) forming an inhomogeneous quasi-periodic surface of the response of the thyristor holding current to the increasing dose of γ -radiation (Fig 10 a), b)). This can be represented especially clearly in the contour graph, Fig. 10 c).

The resulting contour graph is qualitative and makes it possible to visualize the possibility of *quasi-periodic recurrence* of I_{holding} , especially in the 11...18 mA range. At the same time, the probability of observation $I_{\text{holding}} < 11$ mA from a practical point of view, is negligibly low. The probability of $I_{\text{holding}} > 18$ mA is much more probable (Fig. 10 c)).

Visualizing the change of I_{holding} using MathCAD [23] makes it possible to determine the radiation resistance limit for the device under study, i.e. dose of Φ_γ , in which there is a sharp change (deterioration) in the criterion parameter, I_{holding} . In this case, it is $\Phi_\gamma \approx 4.5 \cdot 10^4$ mSv.

The data provided in Fig. 1 and 2 were used to construct the relevant surface. They were reduced to a matrix, Fig. 11 a), and the surface was built using standard Mathcad technology, Fig. 11 b).

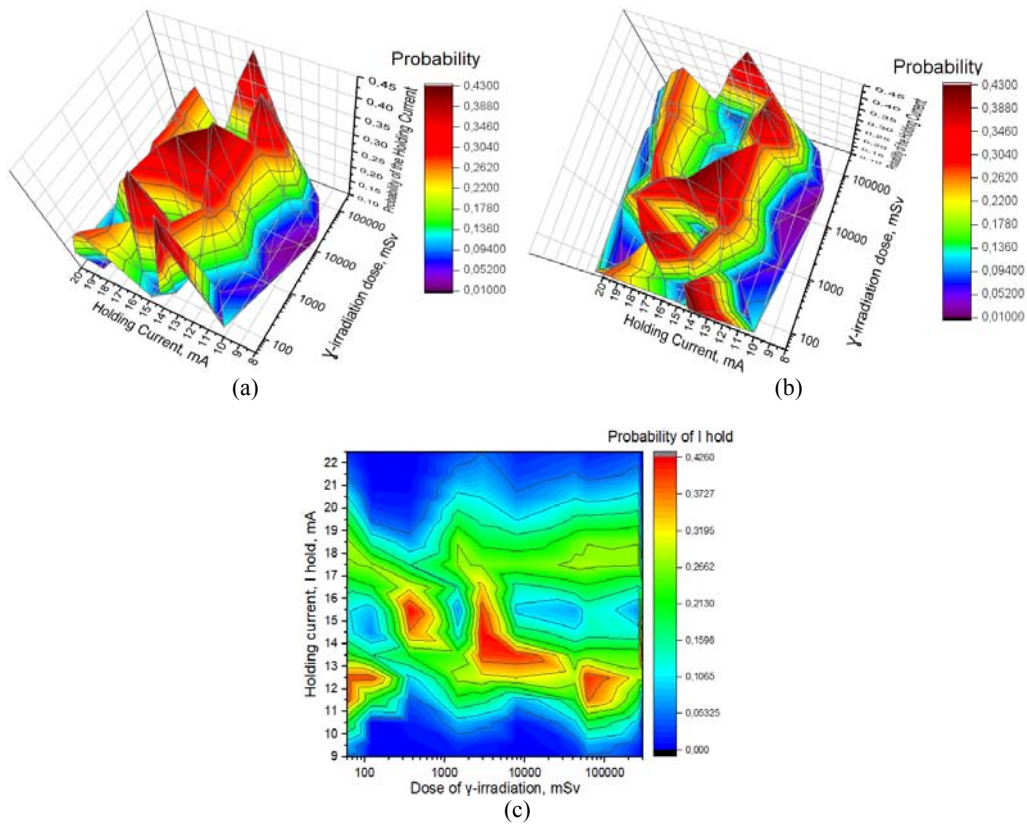


Fig. 10. Quasi-periodic Process of the radiation degradation of the planar npnp structure Holding Current (I_{holding}) under γ -irradiation; a, b) 3d visualization, c) contour plot.

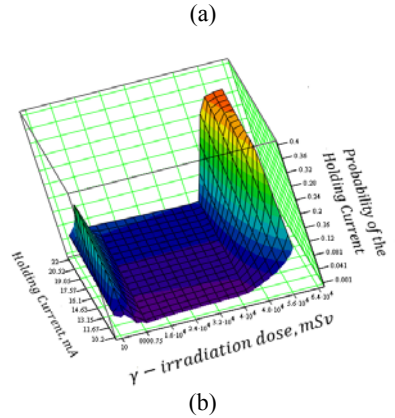
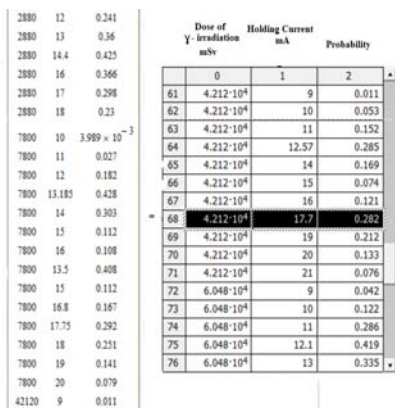


Fig. 11. Increase the likelihood of growth of npnp structure I_{holding} with an increase in the dose of γ -irradiation; a) a fragment of the matrix and a table with data. The range of data for analysis (b)) selected by the *submatrix* command.

The predicted (calculated) numerical value of $I_{\text{holding}}(\Phi_\gamma)$ does not make practical sense as a consequence of the repeatability of numerical values of the holding current at different doses of radiation, but the probability of the Holding Current dependence on the dose of γ -irradiation is easily determined (Fig. 12).

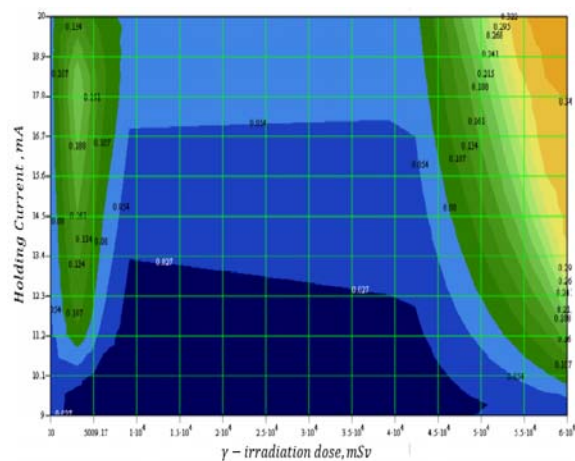


Fig. 12. Nonlinear Probability Change of the holding current, reflecting various Regularities of $I_{\text{holding}}(\Phi_\gamma)$ degradation with an increase in the dose of γ -irradiation.

For example, when $(\Phi_\gamma) \approx 4500$ mSv the probability of the holding current $I_{\text{holding}} = 17.8$ mA is

0.188, and the probability of 11.3 mA is equal to 0.107 or about 1.7 times less.

To design the device, it is logical to use the numerical value $16.7 \leq I_{\text{holding}}(4500 \text{ mSv}) \leq 18.9 \text{ [mA]}$. For higher doses ($\Phi_\gamma \approx 1 \cdot 10^4 \dots 4.5 \cdot 10^4 \text{ mSv}$), it is possible to consider approximately that the Probability of the Holding Current Range changes *stepwise* (Table 1):

Table 1. "Stepwise" Dependence of the Probability of the holding current in the Dose range of γ -irradiation. $\Phi_\gamma = 5 \cdot 10^4 \dots 6 \cdot 10^4 \text{ mSv}$.

No.	Range of Holding Current, I_{holding} , mA	Probability of the Holding Current Range
1.	9.0...13.4	0.027
2..	13.4...16.8	0.054
3	16.8...20.0	0.08

The studied npnp structure has a truly high radiation resistance in the dose range $1 \cdot 10^4 \leq \Phi_\gamma \leq 4.25 \cdot 10^4 \text{ [mSv]}$. In this dose range, the numerical values of the holding current vary in a range approximately equal to $16.9 \leq I_{\text{holding}}(1 \cdot 10^4 \leq \Phi_\gamma \leq 4.25 \cdot 10^4 \text{ [mSv]}) \leq 20.0 \text{ [mA]}$, the probability of these holding currents changes from 0.054 up to 0.08.

At the other doses of γ -irradiation ($\Phi_\gamma \geq 4.5 \cdot 10^4 \text{ mSv}$ and $\Phi_\gamma \leq 1 \cdot 10^4 \text{ mSv}$) the probability of I_{holding} may be an order of magnitude higher (Fig. 12).

From the point of view of assessing the degradation of the npnp structure Holding Current, when $I_{\text{holding}}(\Phi_\gamma)$ approaching the maximum value, of interest, is the visualization of the probability of the holding current in the range $5 \cdot 10^4 \leq \Phi_\gamma \leq 6 \cdot 10^4 \text{ [mSv]}$, Fig. 13.

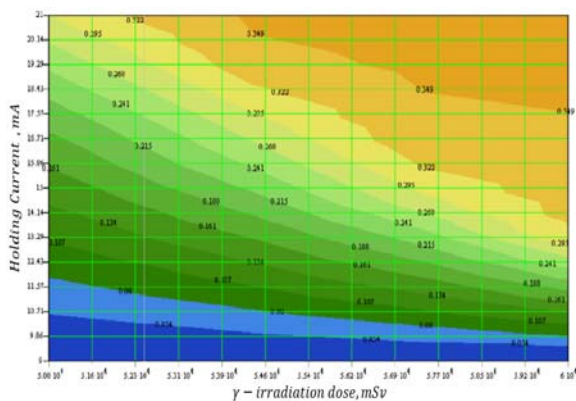


Fig. 13. Probability Increase Feature of I_{holding} ("spiral staircase") when approaching the dose Φ_γ , at which the maximum of Holding Current is achieved.

The probability distribution of numerical values of the Holding Current in the entire studied range of Φ_γ (Fig. 14) indicates the possibility of the existence of

various degradation mechanisms of the I_{holding} at different doses of γ -irradiation. This fact is reflected by two intersecting surfaces.

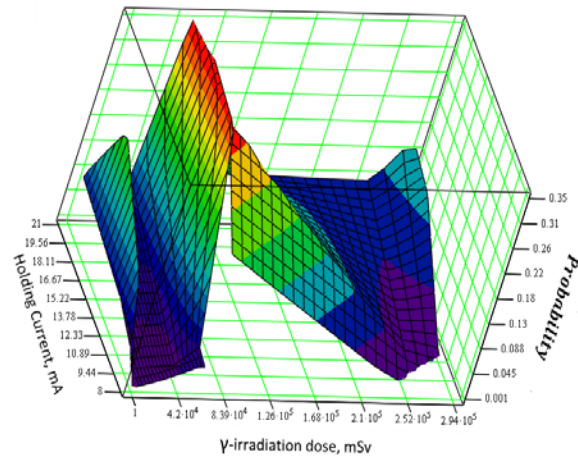


Fig. 14. Visualizing of numerical probabilities of the Holding Current in everything under study range of Φ_γ .

With an accuracy, sufficient for a practical assessment of the radiation resistance of the thyristors of the type under consideration, it is possible to consider, that at $\Phi_\gamma \approx (5.88 \mp 0.7) \cdot 10^4 \text{ mSv}$ there will be a sufficient increase in the probability of $I_{\text{holding}} = 21 \text{ mA}$ (up to 0.349) compared to the likelihood of a "boundary value" of $I_{\text{holding}} \approx 13.8 \text{ mA}$ (0.323), Fig. 15 a).

This value can be considered "borderline" due to the stability of the high probability of holding currents in the "yellow" and "dark-yellow" zones from 0,323 to 0,349. The probability of holding currents less than 13.8 mA ("green" zones with different shades) is significantly lower, equal to 0,296...0,215 and there are no areas with stable probability. Compared to the min value of $I_{\text{holding}} (5.88 \mp 0.7) \cdot 10^4 \text{ mSv}$ is 9 mA, the probability of which is 0.054, the probability of the max value $I_{\text{holding}} ((5.88 \mp 0.7) \cdot 10^4 \text{ mSv}) = \underline{21}$ mA at this dose significantly increase up to 0.349 ($\approx \underline{5.46}$ times).

This phenomenon is also observed at lower γ -irradiation doses but is less pronounced. For example, at $\Phi_\gamma = 3.68 \cdot 10^4 \text{ mSv}$ **probability** $P(21 \text{ mA}) = 0.08$, $P(9 \text{ mA}) = 0.027$. This means that the probability of the max value of I_{holding} exceeds the min value by ≈ 2.96 times. For max $\Phi_\gamma = 2.94 \cdot 10^5 \text{ mSv}$ (Fig. 15 b)) the probability of $I_{\text{holding}} \leq 11 \text{ mA}$ is negligibly small and equal to $2.878 \cdot 10^{-4}$. The experimental observation of such confinement currents is practically impossible. Therefore it is logical to consider, that $I_{\text{holding}} \approx 11 \text{ mA}$ with a probability of 0.027 is the minimum possible holding current at this dose.

The **Probability** of the max value $P(21\text{mA}) = 0.135$, therefore the probability of the max value $I_{\text{holding}} \approx 21 \text{ mA}$ exceeds the min value of $I_{\text{holding}} \approx 11 \text{ mA}$ approximately 5 times: $\left(\frac{0.135}{0.027} = 5\right)$;

The same is true for $I_{\text{holding}} \approx 12.74$ mA with the same probability. The Holding Currents in the other ranges have a probability $\neq 0$ (Table 2).

Table 2. Dependence of the probability of the holding current at the dose range of γ -irradiation $\Phi_{\gamma} \approx 3 \cdot 10^5$ mSv.

No.	Range of Holding Current, I_{holding} , mA	Probability of the Holding Current
1	8.97...10.855	$2.878 \cdot 10^{-4}$
2	10.855...12.74	0.027
3	12.74...14.24	0.054
4	14.24...15.75	0.081
5	15.75...17.25	0.1
6	17.25...20.645	0.135

Due to the difference of zero of holding current probability in the range No 2...6, it may be measured. This means, that the degradation processes, occurring in the thyristor during irradiation, are stochastic.

A sign of stochastic radiation degradation of I_{holding} at $\Phi_{\gamma} \approx 3 \cdot 10^5$ mSv is a gradual increase in the probability of reaching its max value (≈ 21 mA is the probability of the event 13.5 %) and extremely low probability ($2.878 \cdot 10^{-4}$) of $I_{\text{holding}} \leq 11$ mA ("red zone" in Fig. 15, b).

Reaching the I_{holding} max value is also possible with $2.32 \cdot 10^4 \leq \Phi_{\gamma} \leq 2.57 \cdot 10^4$ [mSv], it's the practical failure of the device, but the probability of the event is only ≈ 8 %. The most dangerous dose at which failure is likely ≈ 35 % of the npnp thyristors is $\Phi_{\gamma} = (5.88 \mp 0.7) \cdot 10^4$ mSv.

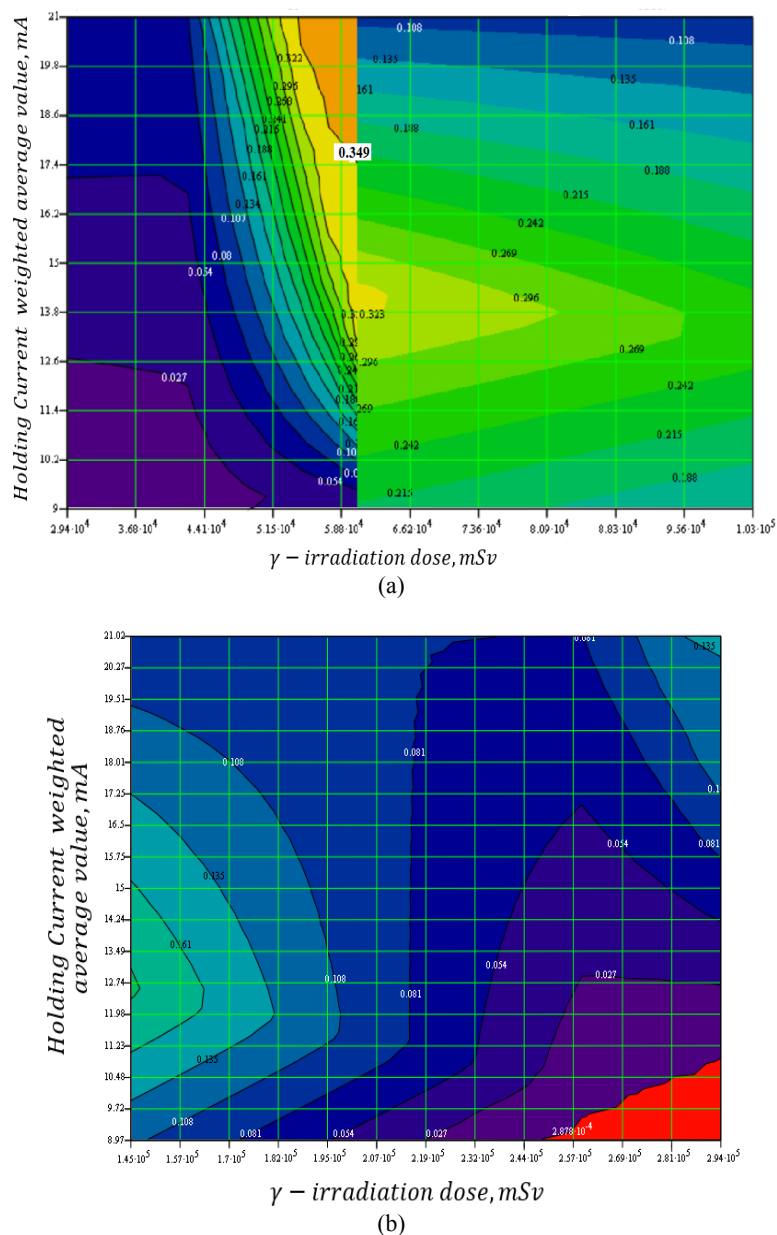


Fig. 15. Changing the probability of numeric values of the Holding Current at different doses of γ - radiation.

4.3. Statistical Estimates of Distribution Parameters, Describing the Holding Current (I_{holding}) Changes of the Thyristors (Low-power npnp Structure) under γ -irradiation at Different Doses

The specific feature of calculating the expected value and variance of the I_{holding} for bimodal distributions (for example, for $\Phi_\gamma = 7800$ mSv), is the calculation of the coefficients for the terms of the probability density functions of the numerical values of the $I_{\text{holding}}(\Phi_\gamma)$.

Let's calculate the probability density function of the holding current at a certain radiation dose, in this case at $\Phi_\gamma = 7800$ mSv. Used (Fig. 16) probability distribution of Holding Current numerical values in the range 9...26 mA.

A brief description of the proposed methodology for calculating the coefficients of distribution peaks in MathCAD is as follows. Using the approach, proposed in [24, p.28], the probability density of the holding current (I_{holding}) numerical values at a given radiation dose may be expressed in the bimodal form (two peaks), formulas (1), (2):

$$f_{\text{probability density}} = k_{\text{left peak}} \cdot f_{\text{left peak } I_{\text{holding}} \text{ probability density}} + \dots + k_{\text{right peak}} \cdot f_{\text{right peak } I_{\text{holding}} \text{ probability density}} \quad (1)$$

$$k_{\text{right peak}} + k_{\text{left peak}} = 1 \quad (2)$$

Calculated the integral likelihood (integral probability) of observing the experimental values of the holding current for thyristors on the control silicon in the entire studied range of $I_{\text{holding}}(\Phi_\gamma)$, i.e. from 9 to 26 mA (3) (the denominator).

Results of the $k_{\text{left peak}}$ and $k_{\text{right peak}}$ calculations are in the same cells.

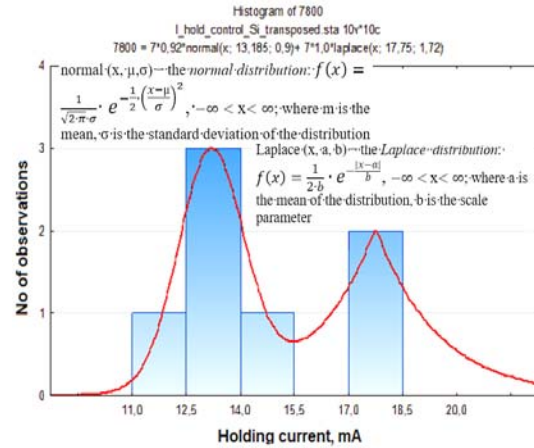
$$\frac{\text{The Denominator (the same for both peaks)}}{=} \int_9^{26} \text{Probability}_{I_{\text{hold_Si}}7800}(I_{\text{hold_Si}}) \cdot dI_{\text{hold_Si}} \quad (3)$$

$$\frac{\text{The Nominator (left peak)}}{=} 0.92 \cdot \int_9^{26} \text{dnorm}(I_{\text{hold_Si}}, 13.185, 0.9) \cdot dI_{\text{hold_Si}} \quad (4)$$

The coefficient of the left peak:

$$\frac{\int_9^{26} 0.92 \cdot \text{dnorm}(I_{\text{hold_Si}}, 13.185, 0.9) \cdot dI_{\text{hold_Si}}}{\int_9^{26} \text{Probability}_{I_{\text{hold_Si}}7800}(I_{\text{hold_Si}}) \cdot dI_{\text{hold_Si}}} = 0.481 \quad (5)$$

Similarly the integral probabilities of the *first (left)* (4), (5) and *second (right)* (6), (7) peaks were calculated (the numerators).



Probability of the I_{holding} at $\Phi_\gamma = 7800$ mSv in the range 9...26 mA:

$$a_{I_{\text{hold}}7800} = 17.75 \quad b_{I_{\text{hold}}7800} = 1.72$$

$$\text{Probability}_{I_{\text{hold_Si}}7800}(I_{\text{hold_Si}}) = 0.92 \cdot \text{dnorm}(I_{\text{hold_Si}}, 13.185, 0.9) + 1.0 \cdot \frac{1}{2 \cdot b_{I_{\text{hold_Si}}7800}} \cdot e^{-\frac{|I_{\text{hold_Si}} - a_{I_{\text{hold_Si}}7800}|}{b_{I_{\text{hold_Si}}7800}}}$$

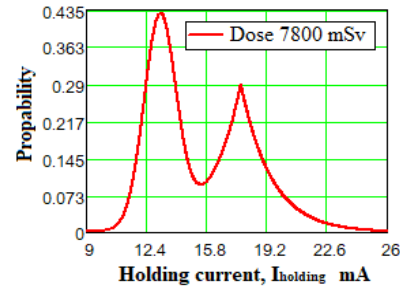


Fig. 16. Sequence for calculating in MathCAD the probability density of the holding current bimodal probability distribution, a) Histogram and distribution function of $I_{\text{holding}}(7800$ mSv); b) formula for calculating the Holding Current Probability of Numerical Values in the range 9...26 mA at the same Φ_γ ; c) visualization of the probability of I_{holding} in the same range.

$$\frac{\text{The Nominator (right peak)}}{=} \int_9^{26} \frac{1}{2 \cdot b_{I_{\text{hold_Si}}7800}} \cdot \left(e^{-\frac{|I_{\text{hold_Si}} - a_{I_{\text{hold_Si}}7800}|}{2 \cdot b_{I_{\text{hold_Si}}7800}}} \right) \cdot dI_{\text{hold_Si}} \quad (6)$$

The coefficient of the right peak:

$$\frac{\int_9^{26} \frac{1}{2 \cdot b_{I_{\text{hold_Si}}7800}} \cdot \left(e^{-\frac{|I_{\text{hold_Si}} - a_{I_{\text{hold_Si}}7800}|}{2 \cdot b_{I_{\text{hold_Si}}7800}}} \right) \cdot dI_{\text{hold_Si}}}{\int_9^{26} \text{Probability}_{I_{\text{hold_Si}}7800}(I_{\text{hold_Si}}) \cdot dI_{\text{hold_Si}}} = 0.519 \quad (7)$$

Then the density of the probability distribution for I_{holding} at $\Phi_\gamma = 7800$ mSv may be expressed as (8).

$$f_{probability_density} = 0.481 \cdot dnorm(I_hold_Si, 13.185, 0.9) + 0.519 \frac{1}{2 \cdot b \cdot I_hold_Si \cdot 7800} \cdot e^{\frac{-|I_hold_Si - a \cdot I_hold_Si \cdot 7800|}{2 \cdot b \cdot I_hold_Si \cdot 7800}} \quad (8)$$

Calculation of the numerical values of the standard parameters, characterizing the resulting distributions, was carried out [25]: weighted average value \bar{X} (mathematical expectation, $M[X]$) experimental results of measurements of the holding current of samples set of npnp thyristors and dispersion $D[X]$ of this physical quantity, where $x \equiv I_{holding}(\Phi_\gamma)$ is a holding current value in the measurement interval, $\varphi(x) \equiv f(I_{holding}(\Phi_\gamma))$ is a density of the probability distribution, formulas (8), (9).

$$\bar{X} = M[X] = \int_{-\infty}^{\infty} x \varphi(x) dx, \quad (9)$$

$$D[X] = \int_{-\infty}^{\infty} (x - M[X])^2 \varphi(x) dx, \quad (10)$$

Application example of $f_{probability_density}$ of $I_{holding}(\Phi_\gamma)$ usage to calculate Holding Current distribution parameters (M_{7800} is a mathematical expectation of I_{hold_Si} at $\Phi_\gamma = 7800$ mSv, D_{7800} is the Holding Current Dispersion), depicted in Listing 1 a), b).

Calculated $I_{holding}(\Phi_\gamma)$ weighted average values and weighted average deviation (square root of dispersion) are in Fig.17, a), b).

a) Weighted average value of $I_{holding}$ at $\Phi_\gamma = 7800$ mSv, M_{7800} :

$$M_{7800} = \int_9^{26} \left(0.481 \cdot dnorm(I_hold_Si, 13.185, 0.9) + 0.519 \frac{1}{2 \cdot b \cdot I_hold_Si \cdot 7800} \cdot e^{\frac{-|I_Si - a \cdot I_hold_Si \cdot 7800|}{2 \cdot b \cdot I_hold_Si \cdot 7800}} \right) I_hold \cdot dI_hold = 15.554 [mA],$$

b) Holding Current Dispersion at $\Phi_\gamma = 7800$ mSv, D_{7800} :

$$D_{7800} = \int_9^{26} \left(0.481 \cdot dnorm(I_hold_Si, 13.185, 0.9) + 0.519 \frac{1}{2 \cdot b \cdot I_hold_Si \cdot 7800} \cdot e^{\frac{-|I_Si - a \cdot I_hold_Si \cdot 7800|}{2 \cdot b \cdot I_hold_Si \cdot 7800}} \right) (I_{hold_Si} - M_{7800})^2 \cdot dI_hold,$$

Weighted average deviation $\sqrt{D_{7800}} = 2.943 [mA]$

Listing 1. Calculation example in Mathcad of the Holding Current ($I_{holding}$, mA) weighted average value at $\Phi_\gamma = 7800$ mSv (a) and its dispersion (b)

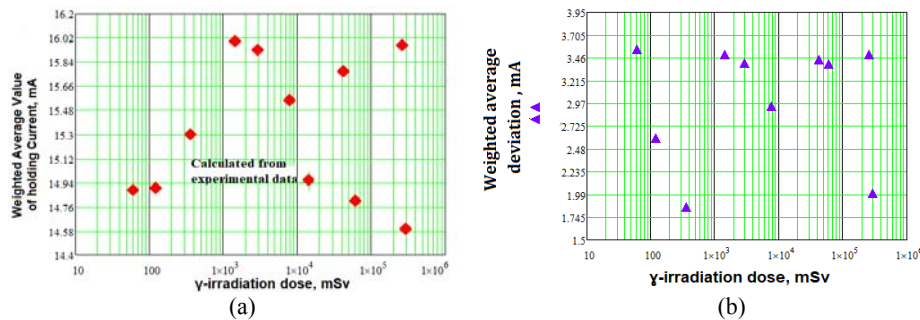


Fig. 17. Dose dependence of the $I_{holding}(\Phi_\gamma)$ weighted average value, a) weighted average deviation (square root of dispersion), b) calculated from experimental data.

From the authors' [26, p. 38] point of view, based on the analysis of publications, concerning the so-called "complex" problems of radiation physics, caused by the combination of nonlinearity and strong non-equilibrium of processes during the irradiation of objects of various natures, in the seemingly complete disorder of an object (the supposedly chaotic distribution of numerical values of the holding current, weighted average deviation), the properties of the hidden order can be manifested.

So, one of the main tasks of modeling was identifying ranges of the γ -irradiation doses which allowed description by an analytic dependence (curve) of experimental $I_{holding}(\Phi_\gamma)$ dependence and the same for holding current dispersion.

5. Quantitative Dependencies, Describing the Holding Current ($I_{holding}$) Degradation at Different γ -irradiation Doses over the Entire Range of Radiation Doses

5.1. Modeling the Dose Dependence of the Holding Current, $I_{holding}(\Phi_\gamma)$

The possibilities of Origin PRO were used to simulate the change in the holding current during irradiation [27]. For example, the results of the calculations of $I_{holding}(\Phi_\gamma)$ at $60 \leq \Phi_\gamma \leq 2000$ mSv are shown in Fig. 18.

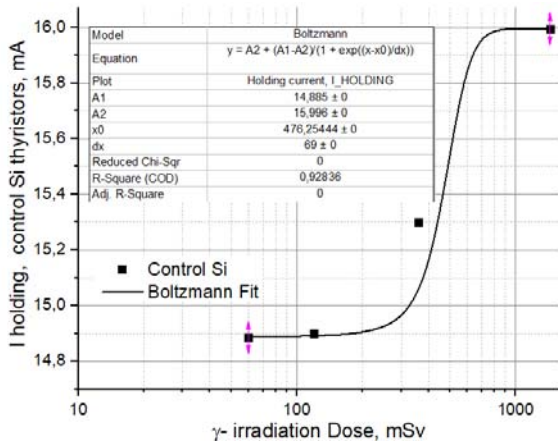


Fig. 18. Origin Pro Approximation Case Study $I_{\text{holding}}(\Phi_\gamma)$ at $60 \leq \Phi_\gamma \leq 2000$ [mSv].

For more simple calculations the resulting Origin PRO models were represented in MathCAD (Listing 2).

The calculation results are shown in Fig. 19. The fully radiation-resistant npnp test structure exists when the irradiation range is $0 \leq \Phi_\gamma \leq 200$ [mSv].

At $200 \leq \Phi_\gamma \leq 1000$ [mSv] there is a "classical" degradation (an increase in the $I_{\text{holding}}(\Phi_\gamma)$), associated with a decrease in the lifetime of injected minority charge carriers due to the recombination processes on radiation defects.

At $\Phi_\gamma \approx 7 \cdot 10^3$ mSv in the base areas of the npnp structure, the formation of radiation defects is expected to be completed. This is indicated by the absence of an $I_{\text{holding}}(\Phi_\gamma)$ change. The strong disequilibrium of the vacancy distribution and the individual characteristics of the impurity-defective composition, which depend on the production technology of certain structures (for example, thyristors or the other types of discrete devices), lead to the possibility of implementing the so-called autocatalytic quasi-chemical reactions between defects [28]. In synergetic systems) anomalously large fluctuations arise. In this case, this is a sample of the devices under study of $I_{\text{holding}}(\Phi_\gamma)$.

The obtained results may be explained using the another concept, described in [28], namely: the possible existence of the intermittency regime, which one shows the coexistence of laminar (smooth) and chaotic (jagged) mechanisms for the accumulation and evolution of radiation defects.

$$Dose_I_hold = 10, 20 \dots 10^6 \text{ mSv}$$

For the range $60 \leq \Phi_\gamma \leq 7000$ [mSv] the form of the equations is the following:

$$\begin{aligned} A1_hold_low_dose &:= 14.885, A2_hold_low_dose := 15.951, \\ x_0_I_hold_low_dose &:= 476.2544, dx_I_hold_low_dose := 69, \\ I_{hold_low_dose_Si}(Dose_I_hold) &:= \\ &= A2_I_hold_low_dose + \frac{(A1_I_hold_low_dose - A2_I_hold_low_dose)}{1 + \exp\left(\frac{(Dose_I_hold) - (x_0_I_hold_low_dose)}{dx_I_hold_low_dose}\right)} \end{aligned}$$

For the range $7000 \leq \Phi_\gamma \leq 3.5 \cdot 10^4$ [mSv] the form of the equations is the following:

$$\begin{aligned} I_{hold_0_high_range_dose_Si_2} &:= 14.27645, I_{hold_x_c_high_range_dose_Si_2} := -19857.9878, \\ I_{hold_w_high_range_dose_Si_2} &:= 43736.68323, I_{hold_A_high_range_dose_Si_2} := 1.69026, \\ I_{hold_0_high_range_dose_Si_2}(Dose_I_hold) &:= \\ &= I_{hold_w_high_range_dose_Si_2} + I_{hold_A_high_range_dose_Si_2} \cdot \\ &\cdot \left[\sin \left[1.071 \cdot \pi \cdot \frac{(Dose_I_hold) - (I_{hold_x_c_high_range_dose_Si_2})}{I_{hold_w_high_range_dose_Si_2}} \right] \right]^2 \end{aligned}$$

For the range $3.584 \cdot 10^4 \leq \Phi_\gamma \leq 9.1 \cdot 10^5$ [mSv] the form of the equations is the following:

$$\begin{aligned} I_{hold_0_high_range_dose_Si_3} &:= 14.594, I_{hold_x_c_high_range_dose_Si_3} := -300, \\ I_{hold_W_high_range_dose_Si_3} &:= 103800, I_{hold_A_high_range_dose_Si_3} := 1.372, \\ I_{hold_high_range_dose_Si_3}(Dose_I_hold) &:= I_{hold_0_high_range_dose_Si_3} + \\ &+ I_{hold_A_high_range_dose_Si_3} \cdot \\ &\cdot \left[\sin \left[\frac{0.52 \cdot \pi \cdot [(Dose_I_hold) - 1 \cdot 10^5] - (I_{hold_x_c_high_range_dose_Si_3})}{(I_{hold_A_high_range_dose_Si_3})} \right] \right]^2 \end{aligned}$$

A simple program may join the obtained equations:

$$\begin{aligned} I_{hold_Si}(Dose_I_hold) &= \\ := \begin{cases} I_{hold_low_dose_Si}(Dose_I_hold) & \text{if } 1 < Dose_I_hold < 2 \cdot 10^3 \\ I_{hold_high_range_dose_Si2}(\{Dose\}I_hold + 0.001) & \text{if } 1.01 \cdot 10^3 < \{Dose_I_hold\} < 3.51 \cdot 10^4 \\ I_{hold_high_range_dose_Si3}(Dose_I_hold) & \text{if } 3.584 \cdot 10^4 < (Dose_I_hold) < 9.1 \cdot 10^5 \end{cases} \end{aligned}$$

Listing 2. The Sequence of Calculation of the Approximating Dependence of the $I_{\text{holding}}(\Phi_\gamma)$ Function.

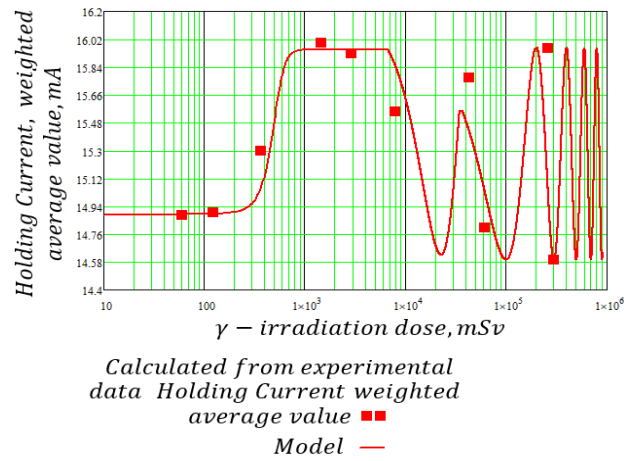


Fig. 19. $I_{\text{holding}}(\Phi_\gamma)$ Curve, Approximating the Weighted Average Value of Holding Current at Different (Φ_γ) .

It's important from the practical approach. The cited work gives an impressive example. Suppose radio equipment or an element base of the electric drive is catastrophically sensitive to these fluctuations.

In that case, quasi-periodicity of failures and return of the equipment to operating condition may occur.

The experimentally shown quasi-periodicity of the change in the holding current at the different Φ_γ indicates different phases of npnp structure degradation.

The existence of chaotic (quasi-periodic) changes indicates an extraordinary evolution of defects in the device, not encountered before.

5.2. Modeling the Dose Dependence of the Holding Current Dispersion, $D_{\text{holding_current}}(\Phi_\gamma)$

The calculation sequence is shown in Listing 3, and the results of the calculation in Fig. 20. Low doses of γ -irradiation also change the physical properties of the npnp structure in a nonlinear manner, within the range of $60 \leq \Phi_\gamma \leq 1000$ mSv there is a peak decline of $D_{\text{holding_current}}(\Phi_\gamma)$. This may indicate a rapid improvement in the crystal structure of thyristor.

A further increase in $\Phi_\gamma > 10^3$ leads to a damped regions with different conductivity types ("low dose effect"). variance oscillation (laminar (smooth) regime). There is a weakly oscillating stabilization of the properties of the Si crystal up to a dose of $\Phi_\gamma \approx 1 \cdot 10^5$ mSv. A chaotic (jagged) regime at $\Phi_\gamma > 1 \cdot 10^5$ mSv may indicate an impending discrete device failure.

Significant reduction in the standard deviation of the Holding Current npnp thyristors is necessary to produce devices for parallel configurations, where good matching of electro-physical characteristics of used Devices is required [29], which can be achieved by reducing the variance of the measured parameters. Min value of standard deviation (≈ 1.85 mA) observed (Fig. 21) at $\Phi_\gamma \approx 350$ mSv and $I_{\text{holding}}(\Phi_\gamma) = 15.3$ mA. This dose can be considered technological,

significantly reducing the spread of numerical values of average-weighted holding currents (decrease of $I_{\text{holding}}(\Phi_\gamma)$ standard deviation).

The observed effect most likely reflects the increase in τ_p (see Section 4.2.1).

6. Conclusions

1. The holding current degradation of a low-power npnp structure under different γ -irradiation doses ($I_{\text{holding}}(\Phi_\gamma)$) occurs non-linearly and is complicated. Shown the quasi-periodicity of the radiation change in the holding current and its dispersion.

2. Obtained experimental data confirm the theoretical approach, proposed in [28], namely: the possible coexistence of laminar (smooth) and chaotic (jagged) phase changes of physical quantity during the irradiation, which is predicted in the cited work.

This work *experimentally* showed the existence of *different phases of $I_{\text{holding}}(\Phi_\gamma)$ degradation*, as well as the similar changes of standard deviation (square root of Dispersion, $D_{\text{holding_current}}(\Phi_\gamma)$).

3. Radiation resistance of npnp structure, understood as the absence of a change of $I_{\text{holding}}(\Phi_\gamma)$ at γ -exposure, is significantly lower than expected and is located in a very narrow range $0 \leq \Phi_\gamma \leq 200$ mSv. At $200 \leq \Phi_\gamma \leq 1000$ mSv S-shape degradation of $I_{\text{holding}}(\Phi_\gamma)$ was observed.

4. From a practical point of view, using such a low-power discrete planar npnp thyristor in the range of $1000 \leq \Phi_\gamma \leq 7 \cdot 10^3$ mSv is advisable. In this very narrow range of Φ_γ holding current $I_{\text{holding}}(\Phi_\gamma)$ is very stable (the "plateau" of numerical values). Dose $\Phi_\gamma \approx 7 \cdot 10^3$ mSv is the beginning of the chaotic (jagged) phase and practically the beginning of the thyristor failure.

5. The given values of $I_{\text{holding}}(\Phi_\gamma)$ are obtained for one type of thyristor and thus are indicative. For *the realistic assessment of the radiation resistance* of *various* types of discrete devices, it is expedient to use the evaluation method used in this work, including the following (see Section 7 of the article).

a) For the range $60 \leq \Phi_\gamma \leq 1000 \text{ mSv}$

$$\begin{aligned} Dose &:= 10, 10 + 10 \cdot 300000, \\ D_{0_Si} &:= 10.375, t_{0_D_Si} := 223.99, x_{c_D_Si} := 80.028, w_{D_Si} := 873.874, A_{D_Si} := -41.992, \\ D_{Si}(Dose) &:= D_{0_Si} + A_{D_Si} \cdot \exp\left[-\frac{Dose}{t_{0_D_Si}}\right] \cdot \sin\left[1.137 \cdot \pi \cdot \left[\frac{Dose}{w_{D_Si}}\right]\right], \end{aligned}$$

b) For the range $1000 \leq \Phi_\gamma \leq 10^5 \text{ mSv}$:

$$\begin{aligned} D_{0_middle_range_dose_Si} &:= 10.01, & W_{middle_range_dose_Si} &:= 12300 \\ t_{0_middle_range_dose_Si} &:= 72698.78101, & A_{middle_range_dose_Si} &:= 0.864488, \\ x_{c_middle_range_dose_Si} &:= -4710, \\ D_{iddle_range_dose_Si}(Dose) &:= \\ = D_{0_middle_range_dose_Si} &+ A_{middle_range_dose_Si} \cdot \exp\left(\frac{-Dose}{t_{0_middle_range_dose_Si}}\right) \cdot \\ \sin\left[0.7002 \cdot \pi \cdot \left(\frac{(Dose+5 \cdot 10^3)-x_{c_middle_range_dose_Si}}{w_{middle_range_dose_Si}}\right)\right], \end{aligned}$$

c) For the range $\Phi_\gamma \geq 10^5 \text{ mSv}$:

$$\begin{aligned} D_{0_high_range_dose_Si} &:= 3.6, x_{c_high_range_dose_Si} := 110000, \\ A_{high_range_dose_Si} &:= 7.5, w_{high_range_dose_Si} := 228000, \\ D_{high_range_dose_Si}(Dose) &:= D_{0_high_range_dose_Si} + A_{high_range_dose_Si} \cdot \\ \cdot \left[\sin\left[2.35 \cdot \pi \cdot \frac{(Dose+6.5 \cdot 10^4)-x_{c_high_range_dose_Si}}{w_{high_range_dose_Si}}\right] \right]^2, \end{aligned}$$

d) Final equation:

$$Dispersion(Dose) := \begin{cases} D_{Si}(Dose) + 0.34, & \text{if } 1 < Dose < 3.38 \cdot 10^3 \\ D_{middle_range_dose_Si}\{Dose\} - 0.1, & \text{if } 2 \cdot 10^3 < Dose < 1.065 \cdot 10^5 \\ D_{high_range_dose_Si}(Dose), & \text{if } 1.085 \cdot 10^5 < Dose < 5.4 \cdot 10^5 \end{cases}$$

Listing 3. Modeling of the Dose Dependence of the Holding Current Dispersion, $D_{\text{holding_current}}(\Phi_\gamma)$.

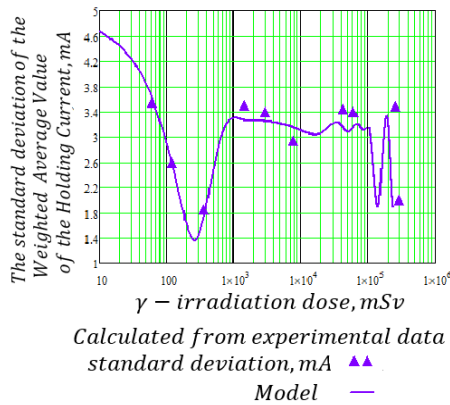


Fig. 20. Non-linear Dose Dependence of the Holding Current Weighted Average Value standard deviation (square root of Dispersion ($D_{\text{holding_current}}(\Phi_\gamma)$)).

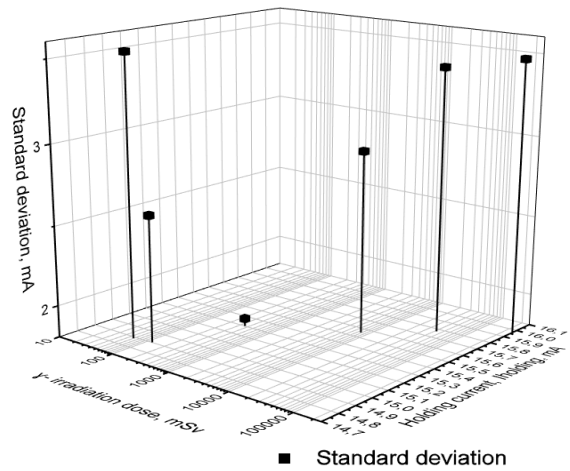


Fig. 21. Nonlinear Relationship of the standard deviation at different γ -irradiation doses.

7. Proposal

For the selected (studied) types of devices, the sample of the studied devices is irradiated with a set of doses of ionizing radiation. Measurements of the chosen parameters are to be carried out, and the experimental results obtained are processed by standard statistical methods (weighted mean, dispersion, standard deviation).

The main point is to construct dose dependences for the selected characteristics of the selected types of devices under study and to construct their approximating dependences to find laminar (smooth) and chaotic (jagged) phases. In our opinion, the laminar phase will show the ranges of real radiation hardness (no changes) and predictable changes of

device parameters under irradiation. The beginning of the chaotic phase indicates the end of the reliable npnp structure operation and the possibility of soon device failure.

References

- [1]. Q. Huang, Investigation of radiation-hardened design of electronic systems with applications to post-accident monitoring for nuclear power plants, <https://ir.lib.uwo.ca/etd/6025>
- [2]. V. Ovchinnikov, et al., Robotics in Chernobyl, *Civil Security Technology*, Vol. 16, Issue 4, 2019, pp. 70-78.
- [3]. R. Smith, et al., Robotic Development for the nuclear environment: challenges and strategy, *Robotics*, Vol. 9, Issue 4, 2020, 94.
- [4]. S. Coloma, et al., The effect of ionizing radiation on robotic trajectory movement and electronic components, *Nuclear Engineering and Technology*, Vol. 55, Issue 11, Nov. 2023, pp. 4191-4203,
- [5]. W. Wang, et al., Robot Protection in the Hazardous Environments, *IntechOpen*, 2017.
- [6]. Solid State Relays (SSR) For Space Applications, <https://www.doeet.com/content/eee-components/actives/solid-state-relays-ssr-for-space-applications/>
- [7]. A. Tasker, Considerations for Designs Using Radiation-Hardened Solid State Relays, Application Note AN-1068, Rev. A, https://www.infineon.com/dgdl/Infineon-Considerations_for_Designs_Using_Radiation-Hardened_Solid_State_Relays-ApplicationNotes-v01_01-EN.pdf?fileId=8ac78c8c84f2c0670184f501f53b1470
- [8]. Electronics Tutorials, Solid State Relay, <https://www.electronics-tutorials.ws/power/solid-state-relay.html>
- [9]. E. I. Yurevich, Fundamentals of Robotics: a Textbook in Specialty "Robots and Robotic Systems", 3rd Ed., :*BHV-Petersburg*, 2010.
- [10]. J. Laifr, Radiation tolerant power electronics for space applications, PhD Thesis, *Czech Technical University in Prague*, November 2018.
- [11]. Dealing with High-Radiation Environments, AVNET, <https://www.avnet.com/wps/wcm/connect/onesite/de21c984-9388-47b0-85cb-d1b02310a936/def-aero-satellite-wp.pdf?MOD=AJPERES&CVID=mXtnMby&CVID=mXtnMby&attachment=true&id=1575672031818>
- [12]. P. Selyshchev. Self-organization of radiation defects: temporal dissipative structures, *International Journal of Engineering, Mathematical and Physical Science*, Vol. 7, Issue 6, 2013, pp. 1050-1053.
- [13]. S. V. Bytkin. Quasi-periodic process of radiation degradation of the planar npnp structure holding current (iholding) under γ -irradiation, in *Proceedings of the 6th International Conference on Microelectronic Devices and Technologies (MicDAT'2024)*, 25-27 September 2024, Ibiza (Balearic Islands), Spain, pp. 5-11.
- [14]. S. Bytkin, Radiation Degradation individual peculiarities of γ -irradiated discrete low power thyristors, manufactured on Si and SiGe, *Sensors & Transducers*, Vol. 263, Issue 4, December 2023, pp. 45-57.
- [15]. MIL-STD-750D Test Methods for Semiconductor Devices. Method 4201.2 Holding Current, USA DoD, https://www.navsea.navy.mil/Portals/103/Documents/NSWC_Crane/SD-18/Test%20Methods/MILSTD750.pdf
- [16]. Passport # 4792 for a sealed gamma-radiation source with Americium-241 radionuclide, type IGIA 5-1, # 346.
- [17]. STATISTICA (Data Analysis Software System), Version 10, <https://www.statsoft.com>
- [18]. P. Selyshchev, Influence of stochastic conditions on self-organization in irradiated materials, *Progress of Theoretical Physics Supplement*, Vol. 150, February 2003, pp. 419-422.
- [19]. A. P. Mamontov, Effect of Small Doses of Ionizing Radiation, 2nd Ed., *Deltaplan*, 2009.
- [20]. P. Taylor, Calculation and Design of Thyristors, *Energoatomizdat*, 1990.
- [21]. A. V. Mostovshchikov, Types of Stored Energy in Solids: Monograph, *Publishing House of Tomsk Polytechnic University*, 2017.
- [22]. S. A. Avdyushkin, I. A. Maksimov, S. G. Kochura, Problematic issues of application of methods of accelerated radiation testing of ECB, *Siberian Aerospace Journal*, Vol. 24, Issue 2, 2023, pp. 280-290.
- [23]. B. Maxfield, Engineering with Mathcad, Using Mathcad to Create and Organize Your Engineering Calculations, *Butterworth-Heinemann*, 2006.
- [24]. R. N. Vadzinsky, Reference Book on Probability Distributions, *Nauka*, 2001.
- [25]. M. A. Kovaleva S. B. Voloshin, Data Analysis. Textbook, *World of Science*, 2019.
- [26]. B. L. Oksengendler, A. Kh. Ashirmetov, F. A. Iskandarova, et al., Interaction of radiation with hierarchical structures, *Surface, X-ray, Synchrotron and Neutron Studies*, Vol. 1, 2023, pp. 37-49.
- [27]. Introduction to Curve Fitting, <https://www.originlab.com/videos/details.aspx?id=36>
- [28]. B. L. Oksengendler, A. F. Zatsepin, A. Kh. Ashirmetov, et al., The concept of "complexity" in radiation physics, *Surface, X-ray, Synchrotron and Neutron Studies*, Vol. 6, 2022, pp. 1-11.
- [29]. Z. Zimek, Application of radiation technologies for the modification of electronic devices, Chapter 21, in *Applications of Ionizing Radiation in Materials Processing* (Y. Sun, A. G. Chmielewski, Eds.), *Institute of Nuclear Chemistry and Technology*, Warszawa, 2017.

